ELSEVIER

Journal of Hepatology 50 (2009) 100–110

Journal of Hepatology

www.elsevier.com/locate/jhep

Activation of lipogenic pathway correlates with cell proliferation and poor prognosis in hepatocellular carcinoma☆

Taro Yamashita[1], Masao Honda[1,2], Hajime Takatori[1], Ryuhei Nishino[1], Hiroshi Minato[3], Hiroyuki Takamura[4], Tetsuo Ohta[4], Shuichi Kaneko[1,*]

[1]*Department of Gastroenterology, Kanazawa University Graduate School of Medical Science, 13-1 Takara-Machi, Kanazawa 920-8641, Japan*
[2]*Department of Advanced Medical Technology, Kanazawa University School of Health Sciences, 13-1 Takara-Machi, Kanazawa 920-8641, Japan*
[3]*Pathology Section, Kanazawa University Hospital, 13-1 Takara-Machi, Kanazawa 920-8641, Japan*
[4]*Department of Gastroenterologic Surgery, Kanazawa University Graduate School of Medical Science, 13-1 Takara-Machi, Kanazawa 920-8641, Japan*

***Background/Aims*: Metabolic dysregulation is one of the risk factors for the development of hepatocellular carcinoma (HCC). We investigated the activated metabolic pathway in HCC to identify its role in HCC growth and mortality.**

***Methods*: Gene expression profiles of HCC tissues and non-cancerous liver tissues were obtained by serial analysis of gene expression. Pathway analysis was performed to characterize the metabolic pathway activated in HCC. Suppression of the activated pathway by RNA interference was used to evaluate its role in HCC *in vitro*. Relation of the pathway activation and prognosis was statistically examined.**

***Results*: A total of 289 transcripts were up- or down-regulated in HCC compared with non-cancerous liver ($P < 0.005$). Pathway analysis revealed that the lipogenic pathway regulated by sterol regulatory element binding factor 1 (*SREBF1*) was activated in HCC, which was validated by real-time RT-PCR. Suppression of *SREBF1* induced growth arrest and apoptosis whereas overexpression of *SREBF1* enhanced cell proliferation in human HCC cell lines. *SREBF1* protein expression was evaluated in 54 HCC samples by immunohistochemistry, and Kaplan–Meier survival analysis indicated that *SREBF1*-high HCC correlated with high mortality.**

***Conclusions*: The lipogenic pathway is activated in a subset of HCC and contributes to cell proliferation and prognosis.**

***Keywords*: Hepatocellular carcinoma; Serial analysis of gene expression; Lipogenesis; Gene expression profiling; Sterol regvulatory element binding factor 1**

Received 26 May 2008; received in revised form 1 July 2008; accepted 23 July 2008; available online 12 October 2008
Associate Editor: J.M. Llovet

☆ The authors who have taken part in the research of this paper declared that they do not have a relationship with the manufacturers of the materials involved either in the past or present and they did not receive funding from the manufacturers to carry out their research.

* Corresponding author. Tel.: +81 76 265 2231; fax: +81 76 234 4250.
E-mail address: skaneko@m-kanazawa.jp (S. Kaneko).

Abbreviations: HCC, hepatocellular carcinoma; *SREBF1*, sterol regulatory element binding factor 1; HBV, hepatitis B virus; HCV, hepatitis C virus; SAGE, serial analysis of gene expression; RT-PCR, reverse transcription-polymerase chain reaction; IHC, immunohistochemistry; FADS1, fatty acid desaturase 1; SCD, stearoyl CoA desaturase; FASN, fatty acid synthase; si-RNA, short interfering-RNA; CLD, chronic liver disease; PCNA, proliferating cell nuclear antigen; IGF, insulin-like growth factor.

1. Introduction

Hepatocellular carcinoma (HCC) is one of the most frequently occurring malignancies in the world [1]. The major risk factors associated with HCC include chronic infection with hepatitis B virus (HBV) and hepatitis C virus (HCV), alcohol abuse, and exposure to aflatoxin B1 [2]. HCC usually develops from liver cirrhosis, which involves continuous inflammation and hepatocyte regeneration, suggesting that reactive oxygen species and DNA damage are involved in the process of hepatocarcinogenesis [3].

The development of gene expression profiling technologies including DNA microarrays and serial analysis

0168-8278/$34.00
doi:10.1016/j.jhep.2008.07.036

of gene expression (SAGE) have enhanced our ability to identify inventory transcripts and global genetic alterations in HCC [4–10]. In general, these methods have demonstrated that transcripts associated with cell growth are up-regulated, whereas those related to inhibition of cell growth are down-regulated, in HCC [11]. It is difficult, however, to decipher molecular pathways activated during hepatocarcinogenesis.

Epidemiological studies suggest that metabolic dysregulation in the liver increases the risk of HCC development. For example, diabetes is associated with a 2-fold increase in the risk of HCC [12]. Obesity and hepatic steatosis also increase the risk of HCC [13–15]. Furthermore, recent studies indicate that HCV infection provokes hepatic steatosis, which may be a vulnerable factor for liver inflammation and HCC development [16,17]. Thus, dysregulation of a metabolic pathway may play a crucial role to promote HCC growth, but the molecular mechanism is still obscure. In this study, we have utilized SAGE [18,19], which enables us to monitor the differential expression of all genes, to determine the global changes in gene expression that occur during hepatocarcinogenesis.

2. Materials and methods

2.1. Tissue samples

All HCC tissues, adjacent non-cancerous liver tissues, and normal liver tissues were obtained from 69 patients who underwent hepatectomy from 1997 to 2005 in Kanazawa University Hospital. Normal liver tissue samples were obtained from patients undergoing surgical resection of the liver for treatment of metastatic colon cancer. HCC and surrounding non-cancerous liver samples were obtained from patients undergoing surgical resection of the liver for the treatment of HCC. The samples used for SAGE, real-time reverse-transcription (RT)-PCR analysis, and immunohistochemistry (IHC) are listed in Supplemental Table 1. All samples used for SAGE and real-time RT-PCR analysis were snap-frozen in liquid nitrogen. Four normal liver tissues and 20 HCCs and their corresponding non-cancerous liver tissues were used for real-time RT-PCR analysis; seven of these HCC samples, along with 47 additional HCC samples, were formalin-fixed paraffin-embedded and used for IHC. HCC and adjacent non-cancerous liver were histologically characterized as described [20].

All strategies used for gene expression analysis as well as tissue acquisition processes were approved by the Ethics Committee and the Institutional Review Board of Kanazawa University Hospital. All procedures and risks were explained verbally, and each patient provided written informed consent.

2.2. SAGE

Total RNA was purified from each homogenized tissue sample using a ToTally RNA extraction kit (Ambion, Inc., Austin, TX), and polyadenylated RNA was isolated using a MicroPoly (A) Pure kit (Ambion). A total of 2.5 μg mRNA per sample was analyzed by SAGE [18]. SAGE libraries were randomly sequenced at the Genomic Research Center (Shimadzu-Biotechnology, Kyoto, Japan), and the sequence files were analyzed with SAGE 2000 software. The size of each SAGE library was normalized to 300,000 transcripts per library, and the abundance of transcripts was compared by SAGE 2000 software. Monte Carlo simulation was used to select genes with significant differences in expression between two libraries without multiple hypothesis testing correction ($P < 0.005$) [21]. Each SAGE tag was annotated using a gene-mapping web site (http://www.ncbi.nlm.nih.gov/SAGE/index.cgi).

2.3. Analysis of signaling networks

Ingenuity Pathways Analysis software (Ingenuity® Systems, www.ingenuity.com) was used to investigate the molecular pathways activated in an HCC SAGE library compared with an adjacent non-cancerous liver SAGE library. All reliable transcripts statistically up-regulated in HCC were investigated and annotated with biological processes, protein-protein interactions, and gene regulatory networks, using a reference-based data file with statistical significance. All identified pathways were screened individually. MetaCore™ software (GeneGo Inc., St. Joseph, MI) was used to evaluate candidate transcription factors responsible for up-regulation of transcripts in HCC.

2.4. RT-PCR

A 1-μg aliquot of each total RNA was reverse-transcribed using SuperScript II reverse-transcriptase (Invitrogen, Carlsbad, CA). Real-time RT-PCR analysis was performed using ABI PRISM 7900 Sequence Detection System (Applied Biosystems, Foster City, CA). Using the standard curve method, quantitative PCR was performed in triplicate for each sample-primer set. Each sample was normalized relative to β-actin. The assay IDs used were Hs00231674_m1 for sterol regulatory element binding factor 1 (*SREBF1*); Hs00203685_m1 for fatty acid desaturase 1 (*FADS1*) ;Hs00748952_s1 for stearoyl CoA desaturase (*SCD*); Hs00188012_m1 for fatty acid synthase (*FASN*); and Hs99999_m1 for β-actin. *SREBF1a* and *SREBF1c* mRNA levels were assayed by semi-quantitative RT-PCR [22].

2.5. RNA Interference targeting SREBF1

Si-RNAs targeting *SREBF1* were constructed using a *Silencer*™ SiRNA Construction kit (Ambion) according to the manufacturer's protocol. We constructed two different si-RNAs, targeting different sites of *SREBF1* (*SREBF1*-1; CAGTGGCACTGACTCTTCC, *SREBF1*-2; TCTACGACCAGTGGGACTG). Control si-RNA duplexes targeting scramble sequences were also synthesized (Dharmacon Research, Inc., Lafayette, CO). Lipofectamine 2000™ reagent (Invitrogen) was used for transfection according to the manufacturer's instructions.

2.6. Cell proliferation assay

Cell proliferation assays were performed using a Cell Titer96 Aqueous kit (Promega, Madison, WI). Results are expressed as the mean optical density (OD) of each five-well set. All experiments were repeated at least twice.

2.7. Soft agar assay

To each well of a six-well plate, containing a base layer of 0.72% agar in growth medium, was added 1×10^4 cells, suspended in 2 ml of 0.36% agar with growth medium (DMEM supplemented with 10% FBS), and the plates were incubated at 37 °C in a 5% CO_2 incubator for 2 weeks. The numbers of colonies in each well were counted as previously described [23].

2.8. TUNEL assay

A DeadEnd™ Colorimetric TUNEL System (Promega) was used to measure nuclear DNA fragmentation as described previously [24].

2.9. Annexin V staining

To evaluate apoptotic cell death, Annexin V binding to cell membranes was evaluated using Annexin V-FITC antibodies and FACSCalibur flow cytometer (BD Biosciences, Franklin Lakes, NJ), as described by the manufacturer.

2.10. Focus assay

HuH7 cells and Hep3B cells were transiently transfected with pCMV7 or pCMV7-*SREBF1c* vectors (kindly provided by Dr. Hitoshi Shimano) using Lipofectamine 2000™ reagent (Invitrogen), as described by the manufacturer. A total of 2×10^3 cells were seeded on six-well plates 48 h after transfection, and cultured in usual media with 400 ng/ml of Geneticin for 9 days. The foci were fixed with ice-cold 100% methanol and stained with 0.5% crystal violet solution. All experiments were performed in triplicates.

2.11. Western blotting

Whole cell lysates were prepared using RIPA lysis buffer. Antibodies used were rabbit polyclonal antibodies to phospho-GSK-3β (ser9) (Cell Signaling Technology Inc., Danvers, MA), rabbit anti-sterol regulatory element binding protein-1 (encoded by *SREBF1*) polyclonal antibody H-160 (Santa Cruz Biotechnology, Inc., Santa Cruz, CA), and β-actin (Sigma–Aldrich Japan K.K., Tokyo, Japan). Immune complexes were visualized by enhanced chemiluminescence (Amersham Biosciences Corp., Piscataway, NJ) as described in the manufacturer's protocol.

2.12. Immunohistochemistry

Rabbit anti-*SREBF1* polyclonal antibody H-160 (Santa Cruz Biotechnology, Inc.) and mouse anti-proliferating cell nuclear antigen (PCNA) monoclonal antibody PC10 (Calbiochem, San Diego, CA) were used to evaluate the immunoreactivity of HCC samples, using a DAKO EnVision+™ Kit, as described by the manufacturer. The signal intensity of *SREBF1* was scored as negative, low, or high determined by the representative staining of the normal liver tissue and cirrhotic liver tissue (Supplemental Fig. 1). HCC was referred as *SREBF1*-high if *SREBF1* expression in the tumor was higher than that in the cirrhotic liver tissue. PCNA index was evaluated as previously described [25].

2.13. Statistical analysis

Kruskal–Wallis test was used to compare the differentially expressed genes, as shown by real-time PCR, among normal liver, CLD, and HCC tissues. Mann–Whitney U test was also used to evaluate the statistical significance of differences of gene expression between CLD and HCC tissues. Spearman's correlation coefficient was used to assess correlations between the expression levels of *SREBF1*, *FADS1*, *SCD*, and *FASN*. Univariate Cox proportional hazards regression analysis was used to evaluate the association of gene expression and clinicopathologic parameters with patient outcomes. All statistical analyses were performed using SPSS software (SPSS software package; SPSS Inc., Chicago, IL) and GraphPad Prism software (GraphPad Software Inc., La Jolla, CA).

3. Results

3.1. Gene expression profiling of HCC

We constructed two SAGE libraries from a HCC–HBV tissue and a corresponding non-cancerous tissue (chronic liver disease (CLD)–HBV). We also used two previously described SAGE libraries, from an HCC–HCV sample and a corresponding non-cancerous tissue sample (CLD–HCV) [4]. After excluding tags detected only once in each library, to avoid the contamination of tags derived from sequence errors, we selected 105,288 tags corresponding to the 9731 genes in all libraries. Using Monte Carlo simulation, we compared the differentially expressed transcripts in HCC and corresponding CLD libraries. Compared with their corresponding CLD libraries, there were statistically significant increases or decreases in 140 transcripts in the HCC–HBV library and in 197 transcripts in the HCC–HCV library ($P < 0.005$).

The HCC–HBV library contained one SAGE tag encoding the HBV–X region, which was increased more than 35-fold compared with its expression in the corresponding CLD–HBV library (Supplemental Table 2). We identified two additional SAGE tags, encoding unknown genes (GTTCTAAAGG, GCATTATGAT), which were expressed more than 10-fold in the HCC–HBV library than in the corresponding CLD–HBV library. The HCC–HBV library also contained tags associated with lipogenesis, at greater than 10-fold abundance, in the HCC–HBV library; these including tags for steroyl-CoA desaturase, fatty acid synthase, and fatty acid desaturase 1.

In contrast, SAGE tags associated with the immune response were up-regulated in the HCC–HCV library. These included tags for Th1-type chemokines, including chemokine ligand 10 (C–X–C motif), chemokine ligand 9 (C–X–C motif), and major histocompatibility complex classes IA and IB (Supplemental Table 3). In addition, tags associated with lipogenesis were increased in the HCC–HCV library, including tags for 3-hydroxy-3-methylglutaryl-coenzyme A synthase 1 and cytochrome P450, family 51, subfamily A, polypeptide 1. Taken together, the differential gene expression patterns may exist in HCC–HBV and HCC–HCV. HBV–X and lipogenesis-related genes are activated in HCC–HBV, whereas genes associated with inflammation as well as lipogenesis are activated in HCC–HCV.

3.2. Analysis of molecular pathways activated in HCC

To further characterize the gene expression patterns of HCC–HBV and HCC–HCV, we performed pathway analysis on SAGE data. Using MetaCore™ software, we found that the candidate transcription factors activated were distinct in each HCC library (Table 1). Several of these transcription factors, including NF-κB, c-Myc, c-Jun, and HNF4-α, have been reported to be activated in HCC [26–29]. In addition, our findings indicated that the transcription factor *SREBF1* may be activated in both HCC–HBV and HCC–HCV (to avoid a confusion, we use HUGO symbol *SREBF1* to indicate both gene/protein name).

Table 1
Candidate transcription factors that regulate molecular pathways activated in HCC.

SAGE library	Transcription factor	Molecular processes	*P*-value
HCC–HCV	NF-κB	Antigen presentation Antigen processing Defense response Immune response	0.004
	SREBF1	Cholesterol biosynthesis Lipid biosynthesis β-Glucoside transport Negative regulation of lipoprotein metabolism	0.05
	SP1	Electron transport; drug metabolism Oxygen and reactive oxygen species metabolism Cell-substrate junction assembly; wound healing	0.05
	IRF1	Immune response Antigen presentation; antigen processing Defense response; positive regulation of cell	0.05
HCC–HBV	HNF4-α	Lipid transport Fatty acid metabolism Smooth muscle cell proliferation	0.002
	HNF1	Acute-phase response; lipid transport Negative regulation of lipid catabolism β-Glucoside transport Negative regulation of lipoprotein metabolism	0.01
	SP1	Zinc ion homeostasis; response to biotic stimulus Nitric oxide mediated signal transduction Copper ion homeostasis; fatty acid biosynthesis	0.01
	c-Jun	Progesterone catabolism; progesterone metabolism Regulation of lipid metabolism; Prostaglandin metabolism	0.03
	C/EBP-α	Lipid transport; negative regulation of lipid catabolism Negative regulation of lipoprotein metabolism β-Glucoside transport Positive regulation of interleukin-8 biosynthesis	0.03
	SREBF1	Lipid biosynthesis; fatty acid biosynthesis Fatty acid metabolism Negative regulation of lipid catabolism Negative regulation of lipoprotein metabolism	0.03
	c-Myc	Fatty acid biosynthesis; fatty acid metabolism Fatty acid desaturation; Activation of pro-apoptotic gene products Release of cytochrome c from mitochondria	0.03
	USF1	Fatty acid metabolism Smooth muscle cell proliferation	0.03
	PPAR-α	Fatty acid metabolism Smooth muscle cell proliferation	0.03
	COUP-TFI	Lipid transport Smooth muscle cell proliferation	0.03
	C/EBP-β	Acute-phase response Regulation of interleukin-6 biosynthesis Fat cell differentiation Inflammatory response	0.03

These findings were evaluated by other pathway analysis software, Ingenuity Pathways Analysis (IPA). We applied the signaling network analysis to the transcripts up-regulated in the HCC libraries ($P < 0.005$). We found that the top signaling network activated in HCC–HBV contained several pathways involved in ERK/MAPK signaling, PPAR signaling, linoleic acid metabolism, and fatty acid metabolism (Supplemental Fig. 2A). Similarly, pathways involved in interferon signaling, NF-κB signaling, antigen presentation, PPAR signaling, linoleic acid metabolism, and fatty acid metabolism were included in the top signaling network activated in HCC–HCV (Supplemental Fig. 2B). Consistent with the results of transcription factor analysis by MetaCore™, pathway analysis indicated that *SREBF1* participates in the lipogenesis pathway in both HCC–HBV and HCC–HCV (blue nodes in Supplemental Fig. 2A and B). *SREBF1*, a major regulator of the lipogenesis pathway, binds to sterol regulatory elements on the genome [30], but less is known about its role in

HCC [31]. We therefore focused on the role of *SREBF1* signaling in HCC.

3.3. Validation of SAGE and signaling network analysis

We performed real-time RT-PCR analysis of *SREBF1* and three representative target genes (*SCD*, *FADS1*, and *FASN*) [20] on 44 samples not used for SAGE. We found that the levels of *SREBF1*, *SCD*, and *FASN* mRNAs were higher in HCC tissues and CLD tissues compared with normal liver, and that these differences were statistically significant (Fig. 1A). We further compared the expression of *SREBF1*, *FADS1*, and *FASN* between HCC and non-cancerous liver tissues, and identified the overexpression of *SREBF1* in HCC with statistical significance (Supplemental Fig. 3). Scatter plot analysis showed that the expression levels of *SREBF1* were correlated with those of *FADS1* ($R = 0.57$, $P < 0.0001$), *SCD* ($R = 0.82$, $P < 0.0001$), and *FASN* ($R = 0.74$, $P < 0.0001$) (Fig. 1B).

Since the mammalian genome encodes two *SREBF1* isoforms, *SREBF1a* and *SREBF1c* [22], we performed semi-quantitative RT-PCR with isoform specific primers to determine which of these isoforms was up-regulated in HCC. We found that *SREBF1c* mRNA, but not *SREBF1a* mRNA, was up-regulated in HCC compared with adjacent non-cancerous liver and normal liver tissues (Supplemental Fig. 4A).

3.4. Functional assay of the lipogenesis pathway in cell lines

Although genome-wide expression profiling showed that the lipogenesis pathway was activated in HCC possibly through up-regulation of *SREBF1*, it was not clear that this pathway played a role in HCC growth. To investigate the role of lipogenesis in HCC cell proliferation, we transfected two short interfering (si)-RNAs (*SREBF1*-1 and *SREBF1*-2) targeting *SREBF1* into the HuH7 and Hep3B cells. These cell lines have no chromosome amplification or deletion on 17p11, on which *SREBF1* is located [32]. Transfection of the si-RNA constructs for *SREBF1*-1 or *SREBF1*-2 decreased expression of *SREBF1* 90% and 70%, respectively, and the expression of both *SCD* and *FADS1* 70% and 60%, respectively (Fig. 2A). Because differences in *SREBF1c* and *SREBF1a* *sequence alignments* are very small, we could not design si-RNAs specifically targeting *SREBF1c*. We therefore checked the effect of si-RNAs on the expression of the *SREBF1* isoforms. We found that the expression of *SREBF1c* was relatively more suppressed than that of *SREBF1a* (Supplemental Fig. 4B), which may have been associated with the higher expression of *SREBF1a* than *SREBF1c* in cultured cell lines [25].

We found that the growth of these transfected cells was significantly inhibited at 72 h compared with mock transfected cells (Fig. 2B and Supplemental Fig.5A). Examination of anchorage independent cell growth showed strong suppression by deactivation of the lipogenesis pathway (Fig. 2C). Because insulin-like growth factor (IGF) is known to induce cancer cell proliferation through activation of PI3-kinase signaling followed by *SREBF1* induction, we investigated the effect of *SREBF1* knockdown on IGF2 mediated cell proliferation. Interestingly, *SREBF1* knockdown abrogated the IGF2 dependent cell proliferation (Supplemental Fig. 5B). Moreover, both the TUNEL assay and annexin V staining showed that transfection of *SREBF1* si-RNAs increased apoptosis compared with mock transfected cells (Fig. 2D and E).

We further investigated the role of *SREBF1* overexpression on cell growth *in vitro*. We transiently transfected control pCMV7 plasmids or pCMV7-*SREBF1c* plasmids (Fig. 3A), and cell proliferation was enhanced in *SREBF1* overexpressing cells compared with the control in both HuH7 and Hep3B cells evaluated by focus assay (Fig. 3B and supplemental Fig. 6). Furthermore, overexpression of *SREBF1* intensified the phosphorylation of GSK-3β, one of the major kinase phosphorylated by the activation of IGF signaling, in a dose-dependent manner (Fig. 3C).

3.5. SREBF1 Expression and prognosis

Since the above results indicated that *SREBF1* signaling may play an important role on tumor cell growth, we investigated the relationship between *SREBF1* expression and mortality in 54 HCC patients by IHC. When we examined the expression of *SREBF1* in HCC tissues and adjacent non-cancerous liver tissues, we identified the increase of the cytoplasmic *SREBF1* staining in a subset of HCC (Fig. 4A). We evaluated the expression of *SREBF1* in HCC and classified 4, 30, and 20 HCCs as *SREBF1*-negative, *SREBF1*-low, and *SREBF1*-high HCC, respectively (Fig. 4B and Supplemental Fig. 1). We could not detect any differences of clinico-pathological characteristics between *SREBF1*-high HCC and *SREBF1*-low/-negative HCC including histological steatosis (Supplemental Table4). Since the seven of these HCC samples were also used for real-time RT-PCR analysis, we investigated the relation of *SREBF1* RNA and protein expression (Fig. 4C). *SREBF1*RNA expression was significantly higher in *SREBF1*-high HCC than in *SREBF1*-low/-negative HCC with statistical significance ($P = 0.03$). Then we examined the cell proliferation of these HCC samples by PCNA staining. Notably, PCNA indexes were significantly higher in *SREBF1*-high HCC than *SREBF1*-low/-negative HCC with statistical significance ($P < 0.001$) (Fig. 4D). We further investigated the relationship between *SREBF1*

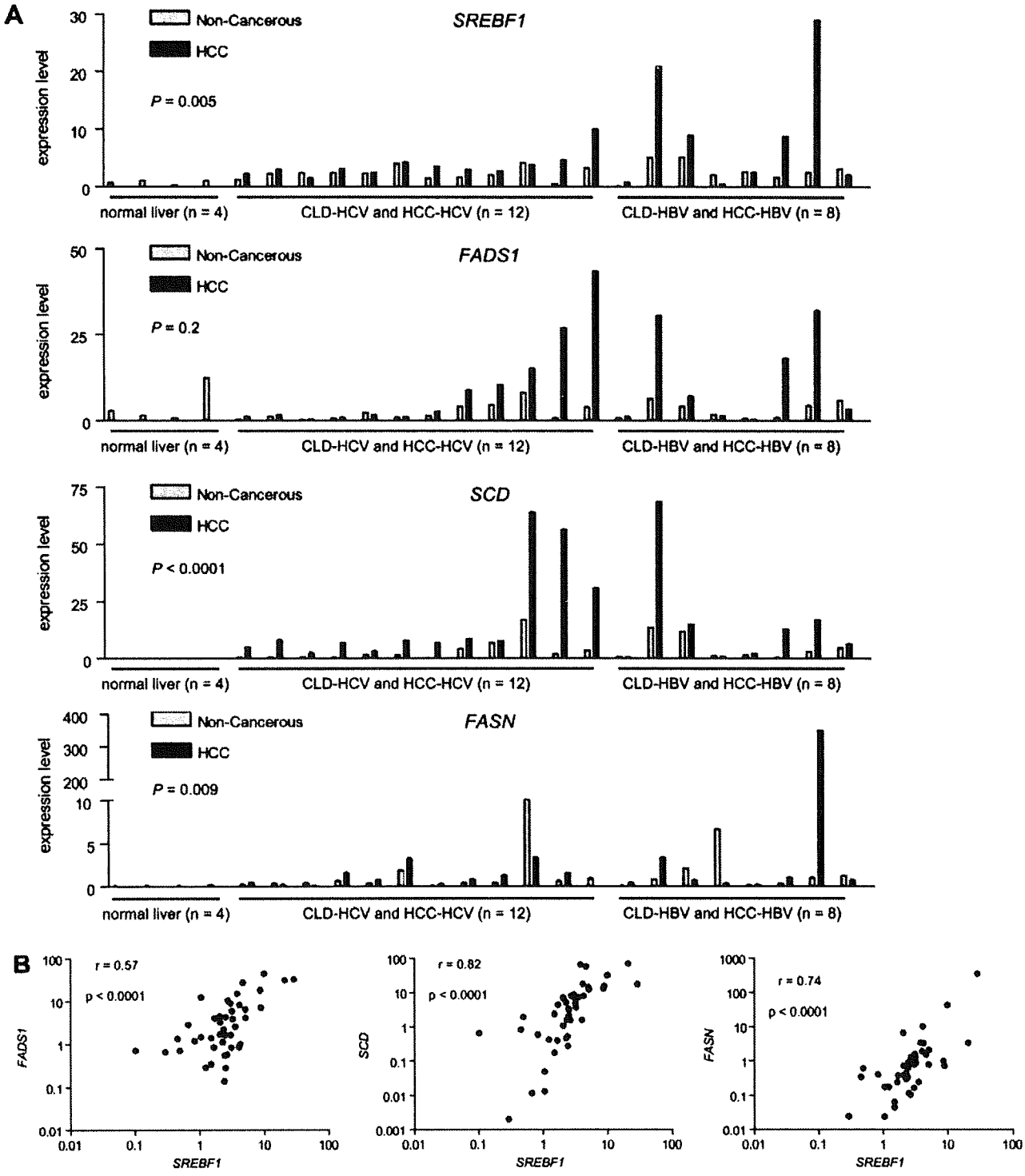

Fig. 1. (A) Real-time quantitative RT-PCR analysis. RNA was isolated from 44 tissue samples: 20 HCC, 20 corresponding CLD, and four normal liver samples. Differential expression of each gene among normal liver tissues, CLD tissues, and HCC tissues was examined by Kruskal–Wallis tests. (B) Scatter plot analysis. Gene expression levels of *FADS1*, *SCD* and *FASN* were well-correlated with those of *SREBF1*, as shown by Spearman's correlation coefficients.

protein expression and prognosis. Kaplan–Meier survival analysis showed a significant relationship between poor survival and high *SREBF1* protein expression ($P = 0.04$; Fig. 4E). Univariate Cox regression analysis showed a correlation between high *SREBF1* protein expression and high risk of mortality with statistical

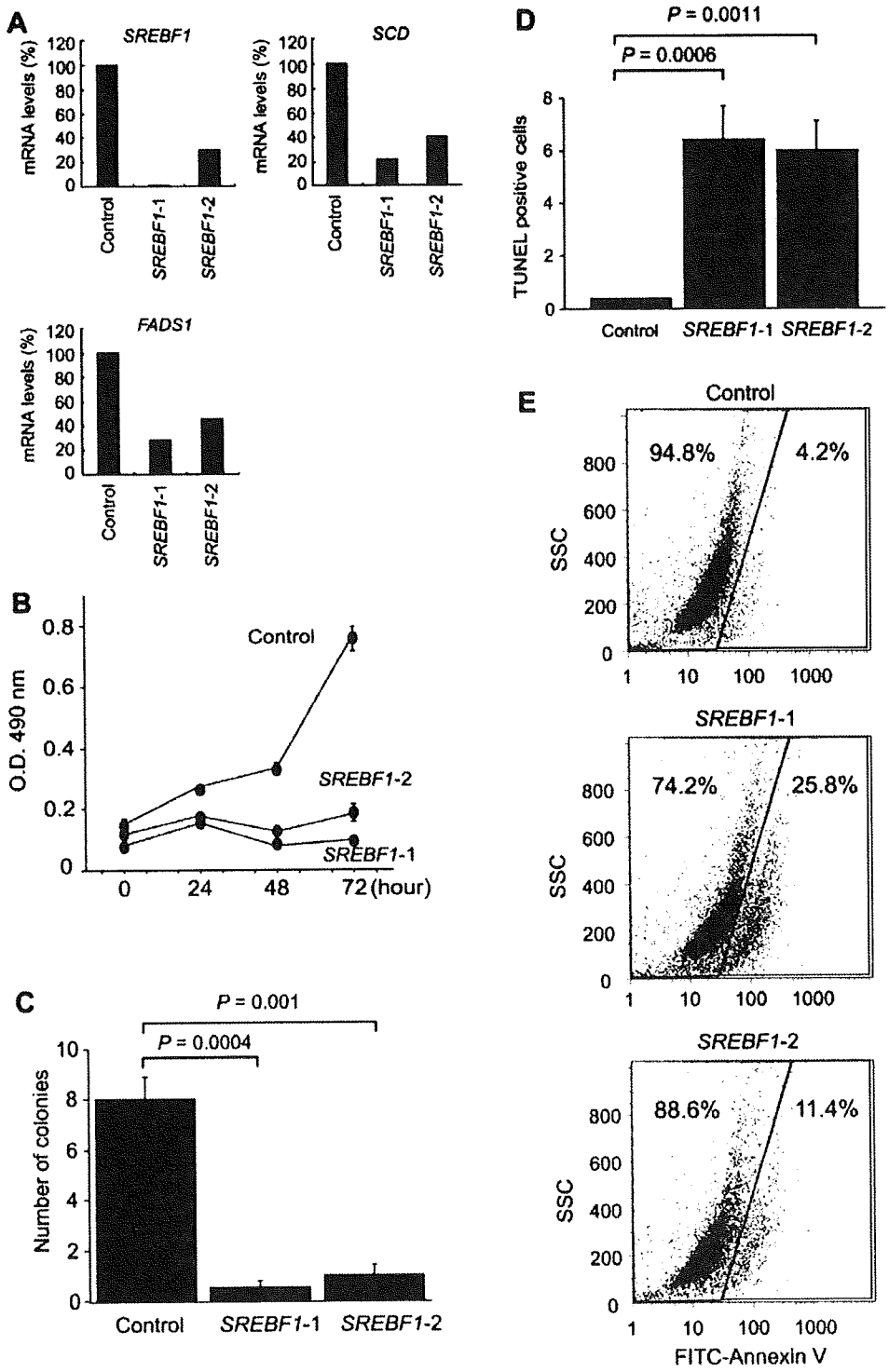

Fig. 2. (A) Effect of RNA interference targeting *SREBF1* in HuH7 cells. Expression levels of *SREBF1* mRNA were reduced by si-RNAs targeting different exons in *SREBF1*. Transcripts of *FADS1* and *SCD* were also down-regulated, showing transcriptional deactivation of the lipogenesis pathway. (B) Cell proliferation assay. Deactivation of the lipogenesis pathway severely reduced cell growth in HuH7 cells. (C) Soft agar assay. Deactivation of the lipogenesis pathway inhibited anchorage independent cell growth in HuH7 cells. (D) TUNEL assay. Deactivation of the lipogenesis pathway significantly increased the number of TUNEL-positive cells in HuH7 cells. (E) Annexin V staining evaluated by flow cytometer. Deactivation of the lipogenesis pathway significantly increased the number of annexin V positive cells in HuH7 cells.

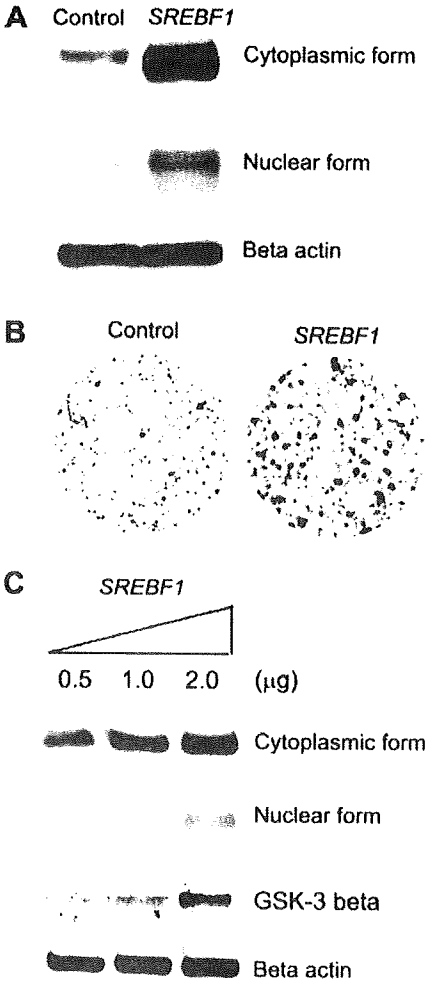

Fig. 3. (A) Western blot analysis of *SREBF1* protein expression in HuH7 cells transfected with control pCMV7 plasmids or pCMV7-*SREBF1c* plasmids. Both cytoplasmic and nuclear forms of *SREBF1* protein expression were increased by pCMV7-*SREBF1c* overexpression. (B) Focus assay of HuH7 cells transfected with control pCMV7 plasmids or pCMV7-*SREBF1c* plasmids. (C) Western blot analysis of *SREBF1* and phospho-GSK-3β protein expression in HuH7 cells transfected with indicated amounts of pCMV7-*SREBF1c* plasmids.

significance (HR, 3.7; 95% CI, 1.0–13.7; $P = 0.05$; Table 2).

4. Discussion

Using large-scale gene expression profiling, we have shown that the lipogenesis pathway is transcriptionally activated in HCC. Our SAGE profiles will be available on our homepage (http://www.intmedkanazawa.jp/) and will be submitted to the Gene Expression Omnibus (http://www.ncbi.nlm.nih.gov/geo/).

We found that the levels of expression of *FADS1*, *SCD*, and *FASN* were each correlated with those of *SREBF1*, suggesting that *SREBF1* is one of the main factors involved in the activation of lipogenesis in HCC. Activation of growth signaling pathways, such as the PI 3-kinase and mitogen-activated protein kinase pathways, has been shown to induce up-regulation of *SREBF1* in prostate and breast cancer cells [33,34]. We have observed induction of *SREBF1* protein expression by IGF2 in HuH7 cells (data not shown). Furthermore, we have identified that *SREBF1* overexpression results in the activation of cell proliferation and PI 3-kinase signaling, whereas expression inhibition of *SREBF1* abrogated the IGF2 induced cell proliferation. Although detailed mechanisms should be clarified in future, our results suggest that *SREBF1* is a key component of PI 3-kinase signaling in HCC.

SREBF1 is induced by alcohol [35], insulin, and fat [30,36], and plays a central role in the mechanism of hepatic steatosis [37]. Interestingly, these *SREBF1* inducers are risk factors for HCC [12,13,38,14]. Strikingly, two recent studies have shown that HBV and HCV infection may also induce hepatic steatosis through activation of *SREBF1* [39,40]. Furthermore, a recent report revealed the activation of *SREBF1* signaling in cancer by hypoxia [41]. Thus, these pathologic conditions such as chronic viral hepatitis, alcohol abuse, obesity, diabetes, and local hypoxia may up-regulate the expression of *SREBF1*, which, in turn, may contribute to an increased risk of hepatocarcinogenesis. Transgenic mice overexpressing *SREBF1* in the liver exhibited hepatic steatosis and hepatomegaly, suggesting the role of *SREBF1* on lipid metabolism and cell proliferation. However, it should be noted that no transgenic mice overexpressing *SREBF1* have been reported to have the risk of HCC development thus far. Interestingly, a recent report indicated that HCV core transgenic mice known to develop HCC showed coordinated activation of lipogenic pathway genes and *SREBF1* [42]. Although further studies are clearly required, we speculate that the activation of *SREBF1* may contribute to promote the development of HCC in already-initiated hepatocytes but not in normal hepatocytes.

Recently, Yahagi et al. reported the activation of lipogenic enzyme related genes in HCC [31]. In that paper, the authors suggested that *SREBF1* expression was not correlated with the expression of other lipogenic genes by Northern blotting, inconsistent with our current data. One possible explanation of these discrepancies might be the different methods for quantitation of mRNA, and we believe that real-time RT-PCR method used in our study would be more accurate. In addition, we evaluated the expression of *SREBF1* and lipogenic genes using more samples (a total of 44 liver and HCC tissues) than Yahagi et al did (10 HCC tissues). Furthermore, a recent paper indicated the coordinated activation of *SREBF1* and lipogenic genes in HCC

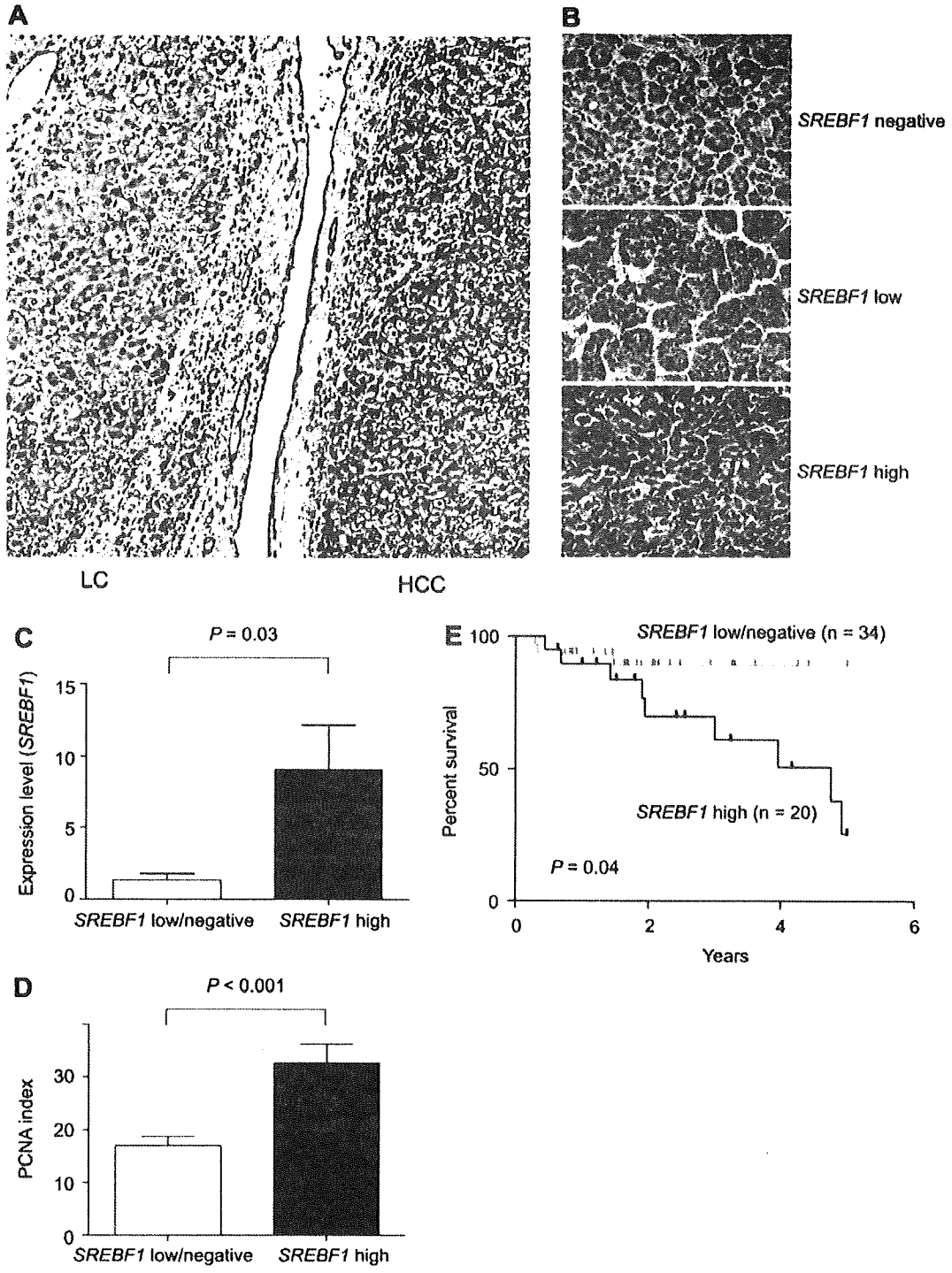

Fig. 4. (A) A photomicrograph of an HCC with adjacent non-cancerous cirrhotic liver stained with anti-*SREBF1* antibodies. (B) Representative photomicrographs of *SREBF1*-negative-, *SREBF1*-low-, and *SREBF1*-high-HCC tissues stained with anti- *SREBF1* antibodies. (C) *SREBF1* gene expression by real-time RT-PCR according to protein expression status assessed by IHC. *SREBF1* was highly expressed in *SREBF1*-high HCC ($P = 0.03$). (D) SREBF1 expression and cell proliferation in HCC. PCNA indexes in *SREBF1*-high HCC were higher than those in *SREBF1*-low/-negative HCC with statistical significance ($P < 0.001$). (E) Kaplan–Meier plots of 54 HCC patients analyzed by immunohistochemistry. The differences between *SREBF1*-high and -low/-negative HCC were analyzed by log-rank test.

developed in the liver of HCV core transgenic mice [42], strongly support our data. Although further studies using large numbers of HCC tissues may be required, these data suggest that the lipogenic gene activation seems to be mediated, at least in part, by *SREBF1* expression in HCC.

Table 2
Univariate Cox regression analysis of survival relative to *SREBF1* protein expression and clinicopathological parameters.

Variables (*n*)	HR (95% CI)	*P*-value
SREBF1 and mortality (n = 54)		
Tumor size		
<3 cm (*n* = 37)	1	
⩾3 cm (*n* = 17)	2.2 (0.6–8.3)	0.2
pTNM stage		
I, II (*n* = 45)	1	
III, IV (*n* = 9)	2.0 (0.4–9.4)	0.4
Serum AFP		
<20 ng/ml (*n* = 35)	1	
⩾20 ng/ml (n = 19)	1.5 (0.4–5.4)	0.5
SREBF1		
Low (*n* = 34)	1	
High (*n* = 20)	3.7 (1.0–13.7)	0.05

Because the majority of our HCC patients analyzed had Child–Pugh class A scores and about 70% had tumors less than 3 cm in diameter, all were expected to have a good prognosis. Indeed, patient survival in this cohort was not segregated by tumor size or pTNM stage (Table 2). Although the sample size was relatively small, we found that enhanced expression of *SREBF1* was a prognostic factor for mortality in HCC possibly due to the highly proliferative nature. Activation of lipogenesis pathways, as shown by overexpression of *FASN*, has been found to correlate with high mortality in breast, prostate, and lung cancer [43], suggesting that activation of lipogenesis may be a fundamental characteristic of cancer with poor prognosis. Thus, *SREBF1* expression may be a good biomarker for HCC classification, a finding that should be validated in a large scale cohort. Because deactivation of the lipogenesis pathway by inhibition of *SREBF1* gene expression could inhibit HCC cell growth *in vitro*, *SREBF1* may be a good target for pharmaceutical intervention in these tumors.

In conclusion, our genome-wide gene expression profiling analyses found that the lipogenesis pathway was activated in a subset of HCC. *SREBF1*, which activates the lipogenesis pathway, may be a good biomarker for HCC prognosis and may be a good target for therapeutic intervention.

Acknowledgements

We are grateful to the members of The Liver Disease Center at Kanazawa University Hospital for providing data of human liver tissue samples. We would also like to thank Dr. Hitoshi Shimano for providing invaluable reagents.

Appendix A. Supplementary data

Supplementary data associated with this article can be found, in the online version, at doi:10.1016/j.jhep.2008.07.036.

References

[1] El-Serag HB, Mason AC. Rising incidence of hepatocellular carcinoma in the United States. N Engl J Med 1999;340:745–750.
[2] Bosch FX, Ribes J, Diaz M, Cleries R. Primary liver cancer: worldwide incidence and trends. Gastroenterology 2004;127:S5–S16.
[3] Wang XW, Hussain SP, Huo TI, Wu CG, Forgues M, Hofseth LJ, et al. Molecular pathogenesis of human hepatocellular carcinoma. Toxicology 2002;181-182:43–47.
[4] Yamashita T, Kaneko S, Hashimoto S, Sato T, Nagai S, Toyoda N, et al. Serial analysis of gene expression in chronic hepatitis C and hepatocellular carcinoma. Biochem Biophys Res Commun 2001;282:647–654.
[5] Shirota Y, Kaneko S, Honda M, Kawai HF, Kobayashi K. Identification of differentially expressed genes in hepatocellular carcinoma with cDNA microarrays. Hepatology 2001;33:832–840.
[6] Okabe H, Satoh S, Kato T, Kitahara O, Yanagawa R, Yamaoka Y, et al. Genome-wide analysis of gene expression in human hepatocellular carcinomas using cDNA microarray: identification of genes involved in viral carcinogenesis and tumor progression. Cancer Res 2001;61:2129–2137.
[7] Xu XR, Huang J, Xu ZG, Qian BZ, Zhu ZD, Yan Q, et al. Insight into hepatocellular carcinogenesis at transcriptome level by comparing gene expression profiles of hepatocellular carcinoma with those of corresponding noncancerous liver. Proc Natl Acad Sci USA 2001;98:15089–15094.
[8] Iizuka N, Oka M, Yamada-Okabe H, Mori N, Tamesa T, Okada T, et al. Comparison of gene expression profiles between hepatitis B virus- and hepatitis C virus-infected hepatocellular carcinoma by oligonucleotide microarray data on the basis of a supervised learning method. Cancer Res 2002;62:3939–3944.
[9] Thorgeirsson SS, Grisham JW. Molecular pathogenesis of human hepatocellular carcinoma. Nat Genet 2002;31:339–346.
[10] Lee JS, Thorgeirsson SS. Genome-scale profiling of gene expression in hepatocellular carcinoma: classification, survival prediction, and identification of therapeutic targets. Gastroenterology 2004;127:S51–S55.
[11] Suriawinata A, Xu R. An update on the molecular genetics of hepatocellular carcinoma. Semin Liver Dis 2004;24:77–88.
[12] El-Serag HB, Tran T, Everhart JE. Diabetes increases the risk of chronic liver disease and hepatocellular carcinoma. Gastroenterology 2004;126:460–468.
[13] Hassan MM, Hwang LY, Hatten CJ, Swaim M, Li D, Abbruzzese JL, et al. Risk factors for hepatocellular carcinoma: synergism of alcohol with viral hepatitis and diabetes mellitus. Hepatology 2002;36:1206–1213.
[14] Ohata K, Hamasaki K, Toriyama K, Matsumoto K, Saeki A, Yanagi K, et al. Hepatic steatosis is a risk factor for hepatocellular carcinoma in patients with chronic hepatitis C virus infection. Cancer 2003;97:3036–3043.
[15] Calle EE, Rodriguez C, Walker-Thurmond K, Thun MJ. Overweight, obesity, and mortality from cancer in a prospectively studied cohort of US adults. N Engl J Med 2003;348:1625–1638.
[16] Walsh MJ, Vanags DM, Clouston AD, Richardson MM, Purdie DM, Jonsson JR, et al. Steatosis and liver cell apoptosis in chronic hepatitis C: a mechanism for increased liver injury. Hepatology 2004;39:1230–1238.

[17] Powell EE, Jonsson JR, Clouston AD. Steatosis: co-factor in other liver diseases. Hepatology 2005;42:5–13.
[18] Velculescu VE, Zhang L, Vogelstein B, Kinzler KW. Serial analysis of gene expression. Science 1995;270:484–487.
[19] Yamashita T, Hashimoto S, Kaneko S, Nagai S, Toyoda N, Suzuki T, et al. Comprehensive gene expression profile of a normal human liver. Biochem Biophys Res Commun 2000;269:110–116.
[20] Desmet VJ, Gerber M, Hoofnagle JH, Manns M, Scheuer PJ. Classification of chronic hepatitis: diagnosis, grading and staging. Hepatology 1994;19:1513–1520.
[21] Polyak K, Xia Y, Zweier JL, Kinzler KW, Vogelstein B. A model for p53-induced apoptosis. Nature 1997;389:300–305.
[22] Yokoyama C, Wang X, Briggs MR, Admon A, Wu J, Hua X, et al. SREBP-1, a basic-helix–loop-helix–leucine zipper protein that controls transcription of the low density lipoprotein receptor gene. Cell 1993;75:187–197.
[23] Wang HC, Chang WT, Chang WW, Wu HC, Huang W, Lei HY, et al. Hepatitis B virus pre-S2 mutant upregulates cyclin A expression and induces nodular proliferation of hepatocytes. Hepatology 2005;41:761–770.
[24] Takeba Y, Kumai T, Matsumoto N, Nakaya S, Tsuzuki Y, Yanagida Y, et al. Irinotecan activates p53 with its active metabolite, resulting in human hepatocellular carcinoma apoptosis. J Pharmacol Sci 2007;104:232–242.
[25] Closset J, Van de Stadt J, Delhaye M, El Nakadi I, Lambilliotte JP, Gelin M. Hepatocellular carcinoma: surgical treatment and prognostic variables in 56 patients. Hepatogastroenterology 1999;46:2914–2918.
[26] Arsura M, Cavin LG, Calvisi DF, Thorgeirsson SS, Eferl R, Ricci R, et al. Nuclear factor-kappaB and liver carcinogenesis. Cancer Lett 2005;229:157–169.
[27] Calvisi DF, Thorgeirsson SS. Molecular mechanisms of hepatocarcinogenesis in transgenic mouse models of liver cancer. Toxicol Pathol 2005;33:181–184.
[28] Eferl R, Ricci R, Kenner L, Zenz R, David JP, Rath M, et al. Liver tumor development. c-Jun antagonizes the proapoptotic activity of p53. Cell 2003;112:181–192.
[29] Xu L, Hui L, Wang S, Gong J, Jin Y, Wang Y, et al. Expression profiling suggested a regulatory role of liver-enriched transcription factors in human hepatocellular carcinoma. Cancer Res 2001;61:3176–3181.
[30] Horton JD, Goldstein JL, Brown MS. SREBPs: activators of the complete program of cholesterol and fatty acid synthesis in the liver. J Clin Invest 2002;109:1125–1131.
[31] Yahagi N, Shimano H, Hasegawa K, Ohashi K, Matsuzaka T, Najima Y, et al. Co-ordinate activation of lipogenic enzymes in hepatocellular carcinoma. Eur J Cancer 2005;41:1316–1322.
[32] Kawaguchi K, Honda M, Yamashita T, Shirota Y, Kaneko S. Differential gene alteration among hepatoma cell lines demonstrated by cDNA microarray-based comparative genomic hybridization. Biochem Biophys Res Commun 2005;329:370–380.
[33] Van de Sande T, De Schrijver E, Heyns W, Verhoeven G, Swinnen JV. Role of the phosphatidylinositol 3′-kinase/PTEN/Akt kinase pathway in the overexpression of fatty acid synthase in LNCaP prostate cancer cells. Cancer Res 2002;62:642–646.
[34] Yang YA, Han WF, Morin PJ, Chrest FJ, Pizer ES. Activation of fatty acid synthesis during neoplastic transformation: role of mitogen-activated protein kinase and phosphatidylinositol 3-kinase. Exp Cell Res 2002;279:80–90.
[35] You M, Fischer M, Deeg MA, Crabb DW. Ethanol induces fatty acid synthesis pathways by activation of sterol regulatory element-binding protein (SREBP). J Biol Chem 2002;277:29342–29347.
[36] Muller-Wieland D, Kotzka J. SREBP-1: gene regulatory key to syndrome X? Ann NY Acad Sci 2002;967:19–27.
[37] Sekiya M, Yahagi N, Matsuzaka T, Najima Y, Nakakuki M, Nagai R, et al. Polyunsaturated fatty acids ameliorate hepatic steatosis in obese mice by SREBP-1 suppression. Hepatology 2003;38:1529–1539.
[38] Marrero JA, Fontana RJ, Su GL, Conjeevaram HS, Emick DM, Lok AS. NAFLD may be a common underlying liver disease in patients with hepatocellular carcinoma in the United States. Hepatology 2002;36:1349–1354.
[39] Kim KH, Shin HJ, Kim K, Choi HM, Rhee SH, Moon HB, et al. Hepatitis B virus X protein induces hepatic steatosis via transcriptional activation of SREBP1 and PPARgamma. Gastroenterology 2007;132:1955–1967.
[40] Waris G, Felmlee DJ, Negro F, Siddiqui A. Hepatitis C virus induces proteolytic cleavage of sterol regulatory element binding proteins and stimulates their phosphorylation via oxidative stress. J Virol 2007;81:8122–8130.
[41] Furuta E, Pai SK, Zhan R, Bandyopadhyay S, Watabe M, Mo YY, et al. Fatty acid synthase gene is up-regulated by hypoxia via activation of Akt and sterol regulatory element binding protein-1. Cancer Res 2008;68:1003–1011.
[42] Tanaka N, Moriya K, Kiyosawa K, Koike K, Gonzalez FJ, Aoyama T. PPARalpha activation is essential for HCV core protein-induced hepatic steatosis and hepatocellular carcinoma in mice. J Clin Invest 2008;118:683–694.
[43] Kuhajda FP. Fatty acid synthase and cancer: new application of an old pathway. Cancer Res 2006;66:5977–5980.

UICC
global cancer control

IJC
International Journal of Cancer

Enhancement of tumor-specific T-cell responses by transcatheter arterial embolization with dendritic cell infusion for hepatocellular carcinoma

Eishiro Mizukoshi[1], Yasunari Nakamoto[1], Kuniaki Arai[1], Tatsuya Yamashita[1], Naofumi Mukaida[2], Kouji Matsushima[3], Osamu Matsui[4] and Shuichi Kaneko[1]

[1] Department of Disease Control and Homeostasis, Graduate School of Medicine, Kanazawa University, Kanazawa, Japan
[2] Division of Molecular Bioregulation, Cancer Research Institute, Kanazawa University, Kanazawa, Japan
[3] Department of Molecular Preventive Medicine, Graduate School of Medicine, Tokyo University, Tokyo, Japan
[4] Department of Radiology, Graduate School of Medicine, Kanazawa University, Kanazawa, Japan

Transcatheter arterial embolization (TAE) destroys a tumor by the induction of necrosis and/or apoptosis and causes inflammation with cytokine production, which may favor immune activation and presentation of tumor-specific antigens. In the current study, we attempted to identify the effect of TAE on tumor-specific T-cell responses and the additional effect of dendritic cell (DC) infusion performed during TAE. The prevalence of tumor antigen-specific T cells was determined by interferon-γ enzyme-linked immunospot analysis using alpha-fetoprotein (AFP) and tumor antigen-derived peptides in 20 and 13 patients with hepatocellular carcinoma (HCC) who received TAE and TAE with DC infusion, respectively. The increased frequency of AFP-specific T cells was observed in 6 of 20 patients after TAE. It was observed more frequently in patients with DC infusion than in those with TAE alone. However, tumor recurrence was not completely prevented in patients albeit displayed enhanced immune responses. The evidence that the enhanced immune responses were transient and attenuated within 3 months was provided in time-course analysis. In conclusion, TAE with DC infusion enhances the tumor-specific immune responses more effectively than TAE alone. Although the effect is not sufficient to prevent HCC recurrence, these results may contribute to the development of novel immunotherapeutic approach for HCC.

Hepatocellular carcinoma (HCC) is one of the most common malignancies and has gained major clinical interest because of its increasing incidence. Although current advances in therapeutic modalities have improved the prognosis of patients with HCC, the survival rate is still unsatisfactory.[1–4] One of the reasons for the poor prognosis is the high rate of recurrence after treatment.[5] Therefore, the development of new antitumor therapies to protect against recurrence is important to improve the prognosis for HCC.

To protect against recurrence, tumor antigen-specific immunotherapy is an attractive strategy. Several recent studies of cancer treatment causing tumor necrosis or apoptosis have shown that they induce the activation of tumor-specific immune responses.[6–10] The mechanism to activate host immune responses against tumors is still unknown; however, several studies *in vitro* or *in vivo* suggest that cytokine production, attracting leukocyte infiltration, increase of tumor antigen uptake by macrophages or dendritic cells (DCs) and release of heat shock protein caused by inflammation at the tumor site are associated with the phenomenon.[11–17]

Transcatheter arterial embolization (TAE) has been used extensively in the Western world and Asia to treat unresectable HCCs.[18–20] Although several previous randomized controlled trials have failed to show a survival benefit in patients treated with TAE compared to untreated patients,[21,22] recent studies demonstrated a survival benefit for TAE *versus* conservative treatment in carefully selected patients.[23–25]

Histological assessment of resected HCC after TAE shows that the treatment induces necrotic and apoptotic changes in the tumor.[26–29] Moreover, it is reported that the serum levels of macrophage-colony stimulating factor and the lipopolysaccharide-stimulated production of interleukin-1 beta, IL-6 and tumor necrosis factor-alpha in peripheral whole blood were increased after TAE.[30–32] Taken together with the previously described knowledge of immune responses after treatment to induce tumor necrosis or apoptosis, these observations support the hypothesis that the induction of apoptotic or necrotic cell death and inflammatory cytokines by TAE favors immune activation and induction of tumor-specific T-cell

Key words: immune response, AFP, CTL, immunotherapy, epitope
Abbreviations: HLA: human leukocyte antigens; IFN: interferon; HCV: hepatitis C virus; ELISPOT: enzyme-linked immunospot; TAE: transcatheter arterial embolization; MRP: multidrug resistance-associated protein; hTERT: human telomerase reverse transcriptase
DOI: 10.1002/ijc.24882
History: Received 17 Feb 2009; Accepted 20 Aug 2009; Online 8 Sep 2009
Correspondence to: Shuichi Kaneko, Department of Disease Control and Homeostasis, Graduate School of Medicine, Kanazawa University, Kanazawa, Ishikawa 920-8641, Japan,
Fax: +81-76-2344250, E-mail: skaneko@m-kanazawa.jp

responses. In a previous study, we also made a preliminary report that immune responses specific for tumor antigens were enhanced after HCC treatments.[7,10] In addition, we have recently developed a new immunotherapeutic approach for HCC using DC infusion performed during TAE, showing the potential to enhance tumor-specific immune responses.[7]

In the current study, we first attempted to identify the effect of TAE for tumor-specific T-cell responses in patients with HCC. Next, we examined the additional effects of DC infusion to the tumor site after TAE. Finally, we analyzed the relationship between clinical characteristics of patients and T-cell responses after TAE and evaluated whether the activation of tumor-specific T-cell responses can prevent HCC recurrence.

Material and Methods

Patient population

The study examined 33 patients with HCC, consisting of 25 men and 8 women ranging from 48 to 83 years old with a mean age of 66 ± 9 years. Twenty patients were treated by TAE. Thirteen patients were treated by TAE with DC infusion as a part of clinical study, which was approved by ethical committee of Kanazawa University Graduate School of Medical Science and registered in September 2003. The patients who received TAE with DC infusion were selected according to the criteria we previously reported.[7] All subjects were negative for Abs to human immunodeficiency virus (HIV) and gave written informed consent to participate in this study in accordance with the Helsinki declaration.

Treatment of hepatocellular carcinoma

HCCs were detected by imaging modalities such as dynamic CT scan, MR imaging and abdominal arteriography. The diagnosis of HCC was histologically confirmed by taking US-guided needle biopsy specimens, surgical resection or autopsy in 18 cases. For the remaining 15 patients, the diagnosis was based on typical hypervascular tumor staining on angiography in addition to typical findings, which showed hyperattenuated areas in the early phase and hypoattenuation in the late phase on dynamic CT.[33] The tumor size was categorized as "small" ($\leq$2 cm) or "large" (>2 cm), and tumor multiplicity was categorized as "multiple" ($\geq$2 nodules) or "solitary" (single nodule). The TNM stage was classified according to the Union Internationale Contre Le Cancer (UICC) classification system (6th version).[34]

Twenty patients were treated by TAE as previously described.[19,35] In brief, after evaluation of the feeding arteries and surrounding vascular anatomy, a microcatheter (Microferret, Cook, Bloomington, IN) was inserted into the segmental or subsegmental artery with a coaxial method using a 0.016-inch guidewire (Radifocus GT wire, Terumo, Tokyo, Japan). A mixture of the anticancer drug and iodized oil was administered, and the feeding artery was embolized with gelatin sponge particles (Gelfoam; Pharmacia Upjohn, Kalamazoo, MI). The mixture of anticancer drug and iodized oil contained 10–30 mg of Epirubicin (Farmorubicin; Kyowa Hakko Kogyo, Tokyo, Japan), 1–3 ml of iodized oil (Lipiodol Ultra Fluide) and 0.5–1.0 ml of iohexol (Omnipaque 300).

Preparation and injection of autologous DCs

DCs were generated as previously described.[7] In 6 patients, DCs were pulsed with 0.1 KE/ml OK-432 (Chugai Pharmaceutical, Tokyo, Japan), which is a biological response modifier derived from the weakly virulent Su strain of Streptococcus pyogenes,[36,37] for 3 days before injection. The cells were harvested for injection; 5×10^6 cells were reconstituted in 5-ml normal saline containing 1% autologous plasma, mixed with gelatin sponge particles and infused through an arterial catheter following iodized oil injection during TAE.

After TAE or TAE with DC infusion, 26 patients received percutaneous tumor ablation by ethanol injection (PEIT), microwave coagulation (MCT) or radiofrequency (RF). Twenty-one patients were diagnosed with complete necrosis of the tumor lesion using dynamic CT after the completion of treatment. Follow-ups were conducted at outpatient clinics using blood tests and dynamic CT every 3 months for 1 year.

Laboratory and virologic testing

Blood samples were tested for HBsAg and HCVAb by commercial immunoassays (Fuji Rebio, Tokyo, Japan). HLA-based typing of PBMC from patients was performed using complement-dependent microcytotoxicity with HLA typing trays purchased from One Lambda. The serum alpha-fetoprotein (AFP) level was measured by enzyme immunoassay (AxSYM AFP, Abbott Japan, Tokyo, Japan), and the pathological grading of tumor cell differentiation was assessed according to the general rules for the clinical and pathologic study of primary liver cancer.[38] The severity of liver disease (stage of fibrosis) was evaluated according to the criteria of Desmet *et al.*[39]

Interferon-γ enzyme-linked immunospot assay

The prevalence of tumor antigen-specific T cells was determined by interferon (IFN)-γ enzyme-linked immunospot (ELISPOT) analysis (Mabtech, Nacka, Sweden) as previously described.[10,40] HLA-A24-restricted AFP-derived peptides (10 μg/ml), which were AFP_{357} (EYSRRHPQL), AFP_{403} (KYIQESQAL) and AFP_{434} (AYTKKAPQL),[10] and 20 μg/ml AFP derived from human placenta (Morinaga Institute of Biological Science, Yokohama, Japan, purity >98%) were added directly to the wells. These 3 AFP-derived peptides could induce CTLs showing cytotoxicity against hepatoma cells and were frequently recognized by PBMCs of patients with HCC as we previously reported,[10] and therefore, we selected them as an immunogenic peptide. The HLA-A24-restricted AFP and CMV-derived peptides were used only for HLA-A24 or A23 positive patients. Other tumor antigen-derived peptides consisted of $MRP3_{503}$ (LYAWEPSFL), $MRP3_{692}$ (AYVPQQAWI), $MRP3_{765}$ (VYSDADIFL), $hTERT_{167}$ (AYQVCGPPL), $hTERT_{324}$

(VYAETKHFL) and hTERT$_{461}$ (VYGFVRACL), which we previously reported that they were useful for analyzing host immune responses to HCC.[40,41]

PBMCs were added to the wells at 3×10^5 cells/well. In the assay using PBMC depleted $CD4^+$ or $CD8^+$ cells, the number of cells was adjusted to 3×10^5 cells/well after the depletion. Depletion of $CD4^+$ or $CD8^+$ cells was performed by MACS separation system using CD4 or CD8 MicroBeads (Miltenyi Biotec, Auburn, CA) in accordance with the manufacturer's instructions. After the depletion, 1×10^6 cells were stained with CD4 and CD8 antibodies (Becton Dickinson, Tokyo, Japan) and analyzed by FACSCalibur (Becton Dickinson, Tokyo, Japan) to confirm the ratio of $CD4^+$ and $CD8^+$ cells. Data analysis was undertaken with CELLQuest™ software (Becton Dickinson, San Jose, CA).

Plates were analyzed with a KS ELISpot Reader (Zeiss, Tokyo, Japan). The number of specific spots was determined by subtracting the number of spots in the absence of antigen. Responses were considered positive if more than 10 specific spots were detected and if the number of spots in the presence of antigen was at least 2-fold greater than the number of spots in the absence of antigen. Negative controls consisted of incubation of PBMCs with a peptide representing an HLA-A24-restricted epitope derived from HIV envelope protein (HIVenv$_{584}$) and were always <5 spots per 3×10^5 cells.[42] The positive controls consisted of 10 ng/ml phorbol 12-myristate 13-acetate (PMA, Sigma) or a CMV pp65-derived peptide (CMVpp65$_{328}$).[43] All peptides used in this study were synthesized at Sumitomo Pharmaceuticals (Osaka, Japan). ELISPOT analysis was performed before and 2–4 weeks after TAE. In patients receiving additional treatment for complete ablation of tumor, analysis was performed just before the additional treatment. An increase of antigen-specific T cells was defined as significant when T-cell responses changed to positive or if the number of spots detected after TAE was at least 2-fold greater than the number of spots detected before treatment.

Statistical analysis

Unpaired Student's *t*-test was used to analyze the effect of variables on immune responses in patients with HCC. Fisher's exact test (2-sided *p*-value) was used to analyze the frequency of positive immune responses in patients between with TAE and TAE with DC infusion.

Results

T-cell responses to AFP in the patients who received TAE

The frequency of AFP-specific T cells before and after TAE was tested *ex vivo* in an IFN-γ ELISPOT assay. The serum AFP level and number of peripheral lymphocytes and antigen-specific T cells are shown in Table 1. Before treatment, 2 patients showed a specific T-cell response to AFP-derived peptides and 3 patients to protein in 20 patients (Patients 1–20). After treatment, a T-cell response to AFP-derived peptides and protein was detected in 4 and 3 patients, respectively.

When an increase of antigen-specific T cells was defined as significant if T-cell responses changed to positive or the number of spots detected after TAE was at least 2-fold greater than the number of spots detected before treatment, 6 of 20 (30%) patients (Patients 4, 6, 7, 11, 18 and 20) showed a significant increasing of AFP-specific T-cell frequency after treatment. It was observed even in the patient (Patients 6, 7 and 18) who had no T cells specific to corresponding AFP-derived peptides before treatment. When a decrease of antigen-specific T cells was defined as significant if T-cell responses changed from positive to negative or the number of spots detected after TAE was less than half of the number of spots detected before treatment, 4 of 20 (20%) patients (Patients 5, 14, 15 and 16) showed a significant decreasing of AFP-specific T-cell frequency after treatment.

AFP-specific IFN-γ-producing T cells were also analyzed by ELISPOT assay using PBMC depleted $CD4^+$ or $CD8^+$ cells to determine what kind of T cells is responsive to whole AFP. Depletion of $CD4^+$ or $CD8^+$ cells was performed by MACS separation system, and the results were confirmed by flow cytometric analysis (Fig. 1*a*). After depletion of $CD4^+$ or $CD8^+$ cells, the ratio of each cell population was decreased to less than 0.1% of PBMCs. The IFN-γ ELISPOT assay showed that IFN-γ-producing T cells against AFP consisted of both $CD8^+$ and $CD4^+$ cells (Fig. 1*b*).

To confirm the effect of TAE for host immune responses to HCC, we also examined the frequency of tumor antigen-specific T cells in 4 patients (Patients 5, 8, 10 and 14) using MRP3- or hTERT-derived peptides that we previously identified as useful for analyzing host immune responses to HCC.[40,41] A significant increasing of MRP3- or hTERT-specific T-cell frequency was observed in all patients after TAE (Table 2).

T-cell responses to AFP in the patients who received TAE with DC infusion

In 13 patients receiving TAE with DC infusion (Patients 21–33), 2 patients showed a specific T-cell response with AFP-derived peptides and 2 patients with protein before treatment (Table 3). After treatment, 8 patients showed a specific T-cell response to AFP-derived peptides and 3 patients to protein.

Next, we compared TAE with DC infusion with TAE alone regarding the effect to AFP-specific immune response. Table 4 shows the clinical features of patients with HCC who received TAE and TAE with DC infusion and they were not statistically different except liver function.

The frequency of patients who showed both positive and increasing T-cell response with AFP-derived peptides or protein after treatment was significantly higher in patients receiving TAE with DC infusion than in those receiving TAE alone ($p = 0.04$) (Fig. 2*a*). On the other hand, the frequency of patients who showed both positive and increasing T-cell

Table 1. T cell response to AFP and AFP-derived peptides by ELISPOT assay before and after TAE

				Before treatment								After treatment							
Patient	HLA	Additional treatment	Complete ablation	AFP (ng/ml)	Lymph. (μl^{-1})	AFP_{357}	AFP_{403}	AFP_{434}	AFP	$CMVpp65_{328}$	TT	AFP (ng/ml)	Lymph. (μl^{-1})	AFP_{357}	AFP_{403}	AFP_{434}	AFP	$CMVpp65_{328}$	TT
1	A2	RF	C	<10	1,600	ND	ND	ND	1	ND	0	<10	1,400	ND	ND	ND	0	ND	1
2	A26,A31	RF	C	61	1,700	ND	ND	ND	0	ND	**13**	23	900	ND	ND	ND	**0**	ND	**0**
3	A11,A26	No	–	100	1,700	ND	ND	ND	5	ND	1	50	1,500	ND	ND	ND	0	ND	0
4	A24	RF	C	18	700	0	7	0	6	0	**25**	16	500	1	**10**	1	1	2	**16**
5	A24,A33	RF	C	2,357	1,200	**13**	2	6	0	**13**	0	700	1,100	2	1	1	0	9	0
6	A24	RF	C	14	1,800	0	0	0	0	0	**42**	<10	1,400	**53**	**27**	**38**	**14**	**36**	**108**
7	A23,A33	No	–	96	500	0	0	0	5	**291**	0	138	800	**46**	0	0	3	**484**	0
8	A24,A26	No	–	142	600	1	0	0	0	0	0	126	500	2	0	0	**0**	**166**	1
9	A2,A24	RF	C	<10	700	6	1	0	0	9	0	<10	700	0	0	0	0	**32**	**15**
10	A24	PEIT	C	<10	1,300	8	4	8	8	**146**	5	<10	1,300	0	1	1	0	1	1
11	A24,A26	PEIT	N	18	1,100	0	0	0	1	ND	0	13	400	0	0	0	**15**	**10**	**55**
12	A24,A33	RF	N	11	800	**3**	2	0	4	**94**	**10**	11	700	0	0	0	0	**24**	**0**
13	A11,A24	PEIT	C	52	1,300	0	2	5	1	2	0	24	1,200	0	0	0	0	0	3
14	A24	RF	C	54	2,400	**25**	5	4	8	**12**	0	67	1,700	0	0	0	0	0	**0**
15	A2,A24	RF	N	62	1,200	0	3	0	**25**	2	3	14	800	0	0	0	8	0	0
16	A3,A24	RF	C	2,876	900	0	1	0	**13**	0	5	3,285	700	0	0	0	0	0	**0**
17	A24,A33	No	–	205	400	4	2	3	2	**26**	9	220	100	2	1	0	1	**39**	1
18	A24,A30	RF	C	18	1,100	4	0	3	8	**14**	7	13	900	1	**16**	1	**5**	**12**	**0**
19	A2,A24	RF	C	330	1,500	2	0	0	0	**18**	1	36	1,100	0	4	0	3	8	1
20	A2,A33	RF	C	10	1,400	ND	ND	ND	**10**	ND	**68**	<10	800	ND	ND	ND	**31**	ND	**101**

Abbreviations: Lymph., number of lymphocytes; RF, radiofrequency ablation; PEIT, percutaneous ethanol injection therapy; No, no treatment; C, completed; N, not completed; –, not determined; ND, not done. The bold letters show the positive responses in ELISPOT assays.

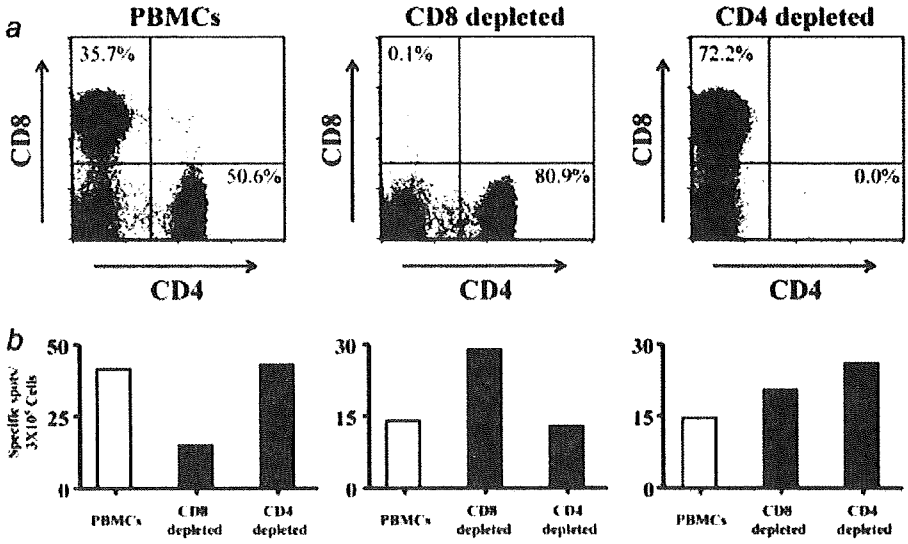

Figure 1. IFN-γ production of CD4- or CD8-depleted T cells against whole AFP. AFP-specific IFN-γ-producing T cells were analyzed by ELISPOT assay using PBMC depleted $CD4^+$ or $CD8^+$ cells to determine what kind of T cells is responsive to whole AFP. Depletion of $CD4^+$ or $CD8^+$ cells was performed by MACS separation system and the results were confirmed by flow cytometric analysis (*a*). IFN-γ ELISPOT assay using nontreated PBMCs and PBMC depleted $CD4^+$ or $CD8^+$ cells showed that T cells producing IFN-γ against whole AFP consisted of both $CD8^+$ and $CD4^+$ cells (*b*). Assays were performed in 5 patients and the representative result is shown.

Table 2. T cell response to other tumor antigen-derived peptides by ELISPOT assay before and after TAE

	Before treatment						After treatment					
Patient	$MRP3_{503}$	$MRP3_{692}$	$MRP3_{765}$	$hTERT_{167}$	$hTERT_{324}$	$hTERT_{461}$	$MRP3_{503}$	$MRP3_{692}$	$MRP3_{765}$	$hTERT_{167}$	$hTERT_{324}$	$hTERT_{461}$
5	2	7	8	0	3.5	7.5	0	0	0	7	3	**35**
8	6	6	1	3	ND	ND	**17**	**18**	**22**	**18**	**14**	9
10	0	1	3	0	5	7	0	4	7	6	**11**	4
14	6	5	0	9	5	**13**	6	14	22	8	**10**	7

Abbreviation: ND, not done. The bold letters show the positive responses in ELISPOT assays.

response with CMV-derived peptide or tetanus toxoid was not different between the 2 groups (Figs. 2*b* and 2*c*).

In the comparison of the mean values of spots generated with AFP-derived peptides, protein, CMV-derived peptides or tetanus toxoid, no significant difference was observed between patients with TAE alone before and after treatment (Figs. 3*a*–3*d*). In contrast, the mean values of spots generated with AFP-derived peptides were significantly higher in patients after TAE with DC infusion than in those before treatment (Fig. 3*e*). The mean values of spots generated with protein, CMV-derived peptides or tetanus toxoid were not significantly different between patients before and after TAE with DC infusion (Figs. 3*f*–3*h*). Based on the above results, we considered that the main difference between TAE alone and TAE with DC infusion was the response to HLA-A24-restricted AFP-derived epitopes. Therefore, to analyze the difference between TAE alone and TAE with DC infusion more precisely, we selected the patients with HLA-A24 or A23 and compared the clinical parameters of both groups. However, there were no statistical differences except liver function in the 2 groups (Table 5).

Enhancement of AFP-specific T-cell responses and treatment outcome

To evaluate the effect of immune enhancement by TAE or TAE with DC infusion for the treatment outcome, we analyzed the clinical course of 17 patients who received complete ablation by additional RFA, PEIT or MCT after these treatments and could be followed up using dynamic CT every 3 months (Table 6). Seven patients showed increasing specific spots for AFP or AFP-derived peptides in ELISPOT assay after TAE. HCC recurrence within 3 months after complete ablation was observed in 3 patients who showed increasing AFP-specific T-cell responses after TAE. Furthermore, recurrence within 6 months after complete ablation was observed

Table 3. T cell response to AFP and AFP-derived peptides by ELISPOT assay before and after TAE with DC infusion

				Before treatment							After treatment							
Patient	HLA	Additional treatment	Complete ablation	AFP (ng/ml)	Lymph. (μl^{-1})	AFP_{357}	AFP_{403}	AFP_{434}	AFP	$CMVpp65_{328}$	TT	AFP (ng/ml)	Lymph. (μl^{-1})	AFP_{357}	AFP_{403}	AFP_{434}	AFP	$CMVpp65_{328}$	TT
21	A24	No	–	332	1,100	7	1	4	ND	10	ND	819	800	11	0	10	ND	188	ND
22	A24,A26	RF	N	341	700	0	26	5	ND	68	ND	237	500	ND	59	ND	ND	81	ND
23	A11,A24	No	–	41	600	0	2	5	1	2	0	43	400	0	0	0	0	0	3
24	A2,A24	MCT	C	1,260	800	3	8	7	ND	19	ND	614	1,300	26	4	7	ND	12	ND
25	A24,A33	RF	C	11	1,500	0	1	0	31	5	15	19	900	1	4	15	26	3	4
26	A24,A33	RF	C	<10	2,000	0	0	0	0	0	0	<10	1,700	0	16	0	0	0	0
27	A24,A26	RF	C	16	700	0	0	0	1	1	0	16	700	2	1	15	9	0	1
28	A11,A31	RF	N	31	800	ND	ND	ND	3	ND	0	33	700	ND	ND	ND	0	ND	0
29	A11,A33	No	–	<10	1,100	ND	ND	ND	0	ND	0	<10	700	ND	ND	ND	0	ND	1
30	A2,A11	RF	C	13	1,300	ND	ND	ND	8	ND	1	14	1,500	ND	ND	ND	12	ND	7
31	A24,A33	RF	C	1,014	800	0	0	0	0	1	0	15	300	0	0	20	0	0	0
32	A11,A24	RF	C	<10	1,000	3	3	11	48	97	0	10	1,200	23	20	20	45	91	23
33	A2,A26	RF	C	29	1,300	ND	ND	ND	0	ND	0	27	1,300	ND	ND	ND	0	ND	0

Abbreviations: Lymph., number of lymphocytes; RF, radiofrequency ablation; PEIT, percutaneous ethanol injection therapy; MCT, microwave coagulation therapy; C, completed; N, not completed; –, not determined; ND, not done. The bold letters show the positive responses in ELISPOT assays.

Table 4. Patient characteristics

	Patients treated by TAE (n = 20)	Patients treated by TAE with DC (n = 13)	p-value[1]
Age (years)[2]	66.6 ± 7.8	65.7 ± 10.0	NS
Sex (M/F)	14/6	11/2	NS
HLA (A23 or 24/others)	16/4	9/4	NS
ALT (IU/l)	51.0 ± 47.4	86.9 ± 62.8	NS
Total bilirubin (g/dl)	1.3 ± 0.9	1.5 ± 0.9	NS
Albumin (g/dl)	3.7 ± 0.7	3.2 ± 0.6	NS
AFP level (ng/ml)	322.7 ± 793.0	239.8 ± 418.2	NS
Diff. degrees of HCC (well/moderate or poor/ND[1])	2/6/12	4/4/5	NS
Tumor size (small/large[3])	4/16	1/12	NS
Tumor multiplicity (multiple/solitary)	18/2	12/1	NS
TNM stage (I, II/III, IV)	19/1	11/2	NS
Histology of nontumor liver (LC/chronic hepatitis)	15/5	10/3	NS
Liver function (Child A/B or C)	14/6	3/10	0.02
Etiology (HCV/HBV/others)	12/2/6	13/0/0	NS

[1]Abbreviations: NS, no statistical significance; ND, not determined. [2]Data are expressed as the mean ± SD. [3]Small: ≤2 cm, large: >2 cm.

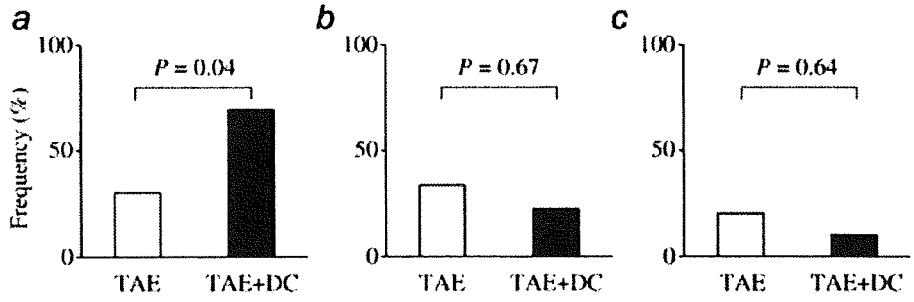

Figure 2. Frequency of the patients who showed enhancement of T-cell responses after treatment. The prevalence of antigen-specific T cells was determined by IFN-γ ELISPOT analysis using alpha-fetoprotein (AFP) and AFP-derived peptides (*a*), CMV pp65-derived peptide (*b*) or tetanus toxoid protein (*c*) in 20 and 13 patients with HCC who received TAE and TAE with DC infusion, respectively.

in 4 and 6 patients who did and did not show increasing AFP-specific T-cell responses, respectively.

Kinetics of AFP-specific T-cell responses before and after TAE

Next, we examined the kinetics of AFP-specific T cells in 8 patients who showed increasing frequency of IFN-γ-producing T cells against AFP or AFP-derived peptides after TAE. The frequency was examined by ELISPOT assay before and 2–4 weeks and 3 months after TAE. Thirteen kinds of AFP-specific T cells showed increasing frequency 2–4 weeks after TAE (Fig. 4); however, the increase was transient and most cell types decreased 3 months after TAE. Three patients showed more than 10 specific spots for AFP or AFP-derived peptides 3 months after TAE (Patients 6, 11 and 30). In analysis of the correlation between the maintenance of AFP-specific T-cell responses and HCC recurrence, 1 patient (Patient 6) had HCC recurrence after 6 months and 1 patient (Patient 30) did not show recurrence. Another patient (Patient 11) did not receive curative ablation and was not analyzed. There was no difference in the kinetics of AFP-specific T cells between patients who received TAE with and without DC infusion.

Discussion

In a previous study, we made a preliminary report that immune responses specific for tumor antigens were enhanced after HCC treatments.[7,10] Similarly, as in our previous or other group's results,[8] we observed enhancement of AFP-specific immune responses in 6 of 20 patients with TAE alone in this study. The enhancement of tumor antigen-specific immune responses was also observed in the cases using MRP3- or hTERT-derived peptides.

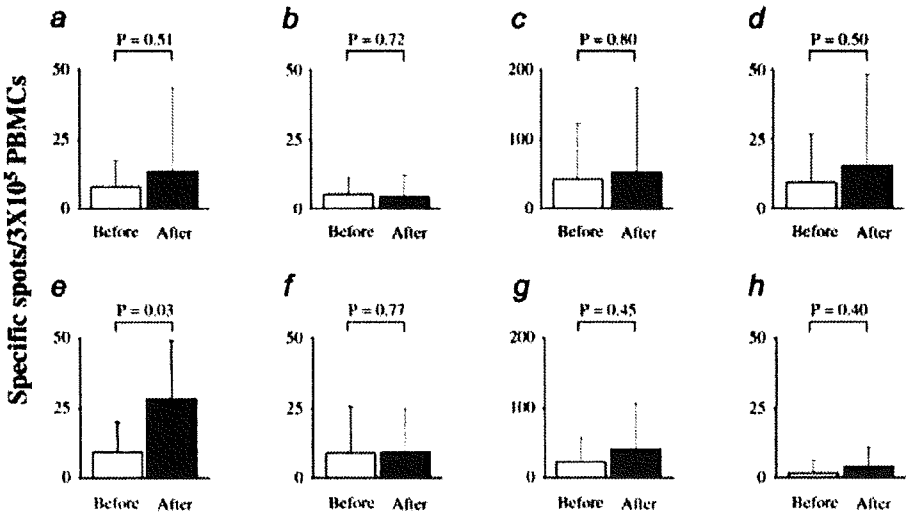

Figure 3. Comparison of direct *ex vivo* analysis (IFN-γ ELISPOT assay) before and after treatment of HCC. The assay was performed using PBMCs of patients who received TAE for AFP-derived peptides (*a*), AFP (*b*), CMV pp65-derived peptide (*c*) or tetanus toxoid protein (*d*). The same assay was performed using PBMCs of patients who received TAE with DC infusion for AFP-derived peptides (*e*), AFP (*f*), CMV pp65-derived peptide (*g*) or tetanus toxoid protein (*h*). AFP and CMV pp65-derived peptides were tested in only HLA-A24 or A23 positive patients. Data are expressed as the mean + SD of specific spots.

Table 5. Characteristics of the patients with HLA-A24 or A23

	Patients treated by TAE (n = 16)	Patients treated by TAE with DC (n = 9)	p-value[1]
Age (years)[2]	65.7 ± 7.8	67.8 ± 10.8	NS
Sex (M/F)	10/6	7/2	NS
ALT (IU/l)	55.9 ± 51.9	75.4 ± 53.0	NS
Total bilirubin (g/dl)	1.4 ± 0.8	1.4 ± 1.1	NS
Albumin (g/dl)	3.6 ± 0.7	3.1 ± 0.6	NS
AFP level (ng/ml)	392.1 ± 877.8	337.2 ± 477.1	NS
Diff. degree of HCC (well/moderate or poor/ND[1])	2/5/9	3/3/3	NS
Tumor size (small/large[3])	3/13	0/9	NS
Tumor multiplicity (multiple/solitary)	15/1	8/1	NS
TNM stage (I, II/III, IV)	15/1	7/2	NS
Histology of nontumor liver (LC/chronic hepatitis)	13/3	8/1	NS
Liver function (Child A/B or C)	10/6	0/9	0.003
Etiology (HCV/HBV/others)	11/1/4	9/0/0	NS

[1]Abbreviations: NS, no statistical significance; ND, not determined. [2]Data are expressed as the mean ± SD. [3]Small: ≤2 cm, large: >2 cm.

The precise mechanism of this phenomenon is still unknown; however, in recent studies, several treatments to destroy tumor cells by necrosis and/or apoptosis have induced antitumor immune responses in animal models[14,44] and even in humans.[6–10] In the study of *in situ* tumor ablation, it is reported that tumor ablation creates a tumor antigen source for the induction of antitumor immunity.[9,44] In another study regarding photodynamic therapy (PDT),[45] it is reported that acute inflammation, expression of heat-shock proteins and providing tumor antigens to DCs caused by PDT induce tumor-specific immune responses.

Based on these results, we hypothesize that DC infusion with TAE can induce antitumor immune responses more effectively than TAE alone. According to DC research in recent years, successful enhancement of the antitumor immune response has been reported by intratumoral

Table 6. Enhancement of AFP-specific T cell response and treatment outcome

	Enhancement of AFP-specific T cell response	Recurrence, 3 months	Recurrence, 6 months
Patient 1	–	N	U
Patient 2	–	N	M
Patient 4	+	M	ND
Patient 5	–	N	M
Patient 6	+	N	U
Patient 9	–	N	M
Patient 10	–	N	N
Patient 13	–	N	N
Patient 14	–	N	N
Patient 16	–	N	M
Patient 19	–	N	U
Patient 24	+	U	ND
Patient 25	+	M	ND
Patient 26	+	N	N
Patient 30	+	N	N
Patient 31	+	N	N
Patient 33	–	N	N

Abbreviations: N, no recurrence; U, uninodular recurrence; M, multinodular recurrence; ND, not determined.

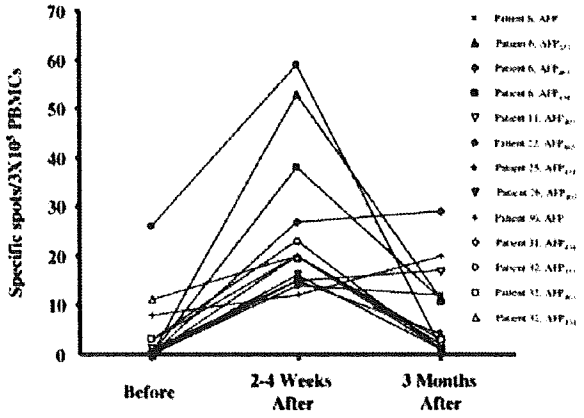

Figure 4. Kinetics of AFP-specific T-cell responses determined by IFN-γ ELISPOT assay before and after TAE. PBMCs were obtained before and 2–4 weeks and 3 months after TAE. Each graph indicates the kinetics of T cells specific for each antigen in each patient. Some patients received additional treatments as indicated in Tables 1 and 3 for a curative treatment after the measurement of T-cell responses at 2–4 weeks after TAE.

administration of DC in combination with tumor ablation.[46,47] Furthermore, immunotherapies using DC have been performed in patients with HCC and their antitumor effects are reported.[48–50] These results support our hypothesis and therefore, in the next step, we examined the immunological effects of DC infusion with TAE.

The comparison of frequency in patients who showed enhancement of AFP-specific immune responses revealed more frequency in patients with DC infusion than in those with TAE alone. On the other hand, there were no differences in the 2 groups in the comparison of frequency for patients who showed enhancement of CMV or TT-specific immune responses. These results suggest that DC infusion with TAE affects tumor-specific immune responses and that the effects are limited to the tumor area.

Some patients with TAE alone showed disappearance of AFP- or control antigen-specific T cells. Although the mechanism of this phenomenon is unknown, anticancer drugs used in TAE might suppress the immune responses, because most of the patients showed decreasing the number of lymphocytes after TAE. These results suggest that TAE alone might give a chance to enhance tumor-specific T-cell responses in only some patients. Further analysis using many more patients with TAE is necessary to make clear the differences in the patients with and without enhancement of T-cell responses. In contrast, disappearance of AFP- or control antigen-specific T cells was not observed in the patients with DC infusion, suggesting strong immunostimulating effect of this treatment.

In analysis of the association between the enhancement of AFP-specific T cells and clinical responses, no correlation could be shown, suggesting that enhancement of T-cell response associated with TAE or TAE with DC infusion may not have protective effect against HCC recurrence. To clarify the mechanism in more detail, we examined the kinetics of AFP-specific T-cell response. Increased frequency of AFP-specific T cells was transient and fell in 4 of 8 patients 3 months after treatment (Fig. 4). Similar to our results, Ayaru *et al.* also reported that the frequency of AFP-specific $CD4^+$ T cells fell in all patients by 1–3 months after TAE.[8] In addition, our results suggest that DC infusion with TAE is not effective to maintain the increased frequency of AFP-specific T cells.

Recent genome profiling studies of HCC show that HCC is a very heterogenous tumor.[51] Furthermore, HCC has multicentric carcinogenesis and develops at different time points. These characters of HCC may also be another reason for no correlation between the enhancement of AFP-specific T cells and clinical responses. The identification of many more tumor antigens and their T-cell epitopes is necessary for more precise analysis of the relationship between antitumor immune response and clinical response, and for immunotherapy.

In the recent study, it is reported that $CD8^+$ T-cell response to AFP is multispecific and AFP-specific IFN-γ-producing $CD8^+$ T cells are directed against different epitopes spreading over the entire AFP sequence with no single